Kummerow, C., Barnes, W., Kozu, T., Shiue, J., and Simpson, J., 1998. The tropical rainfall measuring mission (TRMM) sensor package. *Journal of Atmospheric and Oceanic Technology*, **15**, 809–817.
Llewellyn-Jones, D. T., Minnett, P. J., Saunders, R. W., and Závody, A. M., 1984. Satellite multichannel infrared measurements of sea-surface temperature of the N.E. Atlantic ocean using AVHRR/2. *Quarterly Journal of the Royal Meteorological Society*, **110**, 613–631.
May, D. A., Parmeter, M. M., Olszewski, D. S., and McKenzie, B. D., 1998. Operational processing of satellite sea surface temperature retrievals at the naval oceanographic office. *Bulletin of the American Meteorological Society*, **79**, 397–407.
Merchant, C. J., and LeBorgne, P., 2004. Retrieval of sea surface temperature from space, based on modeling of infrared radiative transfer: capabilities and limitations. *Journal of Atmospheric and Oceanic Technology*, **21**, 1734–1746.
Merchant, C. J., Harris, A. R., Maturi, E., and MacCallum, S., 2005. Probabilistic physically based cloud screening of satellite infrared imagery for operational sea surface temperature retrieval. *Quarterly Journal of the Royal Meteorological Society*, **131**, 2735–2755.
Merchant, C.J., Harris, A.R., Roquet, H., & Le Borgne, P., 2009. Retrieval characteristics of non-linear sea surface temperature from the Advanced Very High Resolution Radiometer. *Geophysical Research Letters*, **36**, L17604. doi:10.1029/2009GL039843.
Minnett, P. J., 1995. The along-track scanning radiometer: instrument details. In Ikeda, M., and Dobson, F. (eds.), *Oceanographic Applications of Remote Sensing*. Boca Raton: CRC Press, pp. 461–472.
Minnett, P. J., 2007. Heat in the ocean. In King, M. D., Parkinson, C. L., Partington, K. C., and Williams, R. G. (eds.), *Our Changing Planet, the View from Space*. Cambridge: Cambridge Univesity Press, pp. 156–161.
Minnett, P. J., Smith, M., and Ward, B., 2011. Measurements of the oceanic thermal skin effect. *Deep Sea Research Part II: Topical Studies in Oceanography*, **58**, 861–868.
Noyes, E. J., Minnett, P. J., Remedios, J. J., Corlett, G. K., Good, S. A., and Llewellyn-Jones, D. T., 2006. The accuracy of the AATSR sea surface temperatures in the Caribbean. *Remote Sensing of Environment*, **101**, 38–51.
O'Carroll, A. G., Eyre, J. R., and Saunders, R. W., 2008. Three-way error analysis between AATSR, AMSR-E, and in situ sea surface temperature observations. *Journal of Atmospheric and Oceanic Technology*, **25**, 1197–1207.
Philander, S. G. (ed.), 1989. *El Niño, La Niña, and the Southern Oscillation*. San Diego: Academic. International Geophysics Series.
Prata, A. J. F., Cechet, R. P., Barton, I. J., and Llewellyn-Jones, D. T., 1990. The along-track scanning radiometer for ERS-1 – scan geometry and data simulation. *IEEE Transactions on Geoscience and Remote Sensing*, **28**, 3–13.
Reynolds, R. W., 1993. Impact of Mount Pinatubo aerosols on satellite-derived sea surface temperature. *Journal of Climate*, **6**, 768–774.
Saunders, R. W., and Kriebel, K. T., 1988. An improved method for detecting clear sky and cloudy radiances from AVHRR data. *International Journal of Remote Sensing*, **9**, 123–150. Correction, 1988, International Journal of Remote Sensing, 9, 1393–1394.
Shay, L. K., Goni, G. J., and Black, P. G., 2000. Effects of a warm oceanic feature on Hurricane Opal. *Monthly Weather Review*, **128**, 1366–1383.
Walton, C. C., Pichel, W. G., Sapper, J. F., and May, D. A., 1998. The development and operational application of nonlinear algorithms for the measurement of sea surface temperatures with the NOAA polar-orbiting environmental satellites. *Journal of Geophysical Research*, **103**, 27999–28012.
Wentz, F. J., and Meissner, T., 2000. *AMSR Ocean Algorithm (ATBD), Version 2*. Santa Rosa: Remote Sensing Systems.
Wentz, F. J., Gentemann, C., Smith, D., and Chelton, D., 2000. Satellite measurements of sea-surface temperature through clouds. *Science*, **288**, 847–850.
Wentz, F., Gentemann, C. L., and Ashcroft P., 2003. On-orbit calibration of AMSR-E and the retrieval of ocean products. In *12th Conference on Satellite Meteorology and Oceanography*, American Meteorological Society, Long Beach.

Cross-references

Calibration, Microwave Radiometers
Calibration, Optical/Infrared Passive Sensors
Climate Data Records
Climate Monitoring and Prediction
Microwave Radiometers
Optical/Infrared, Atmospheric Absorption/Transmission, and Media Spectral Properties
Optical/Infrared, Radiative Transfer
Thermal Radiation Sensors (Emitted)

SEA SURFACE WIND/STRESS VECTOR

W. Timothy Liu and Xiaosu Xie
Jet Propulsion Laboratory, California Institute of Technology, Pasadena, CA, USA

Definition

Wind is air in motion and is basically a vector quantity with a magnitude (speed) and a direction. Ocean surface stress is another vector quantity closely related to wind; it is the turbulent transfer of momentum between the ocean and the atmosphere. Their different applications are summarized in the section "Scientific significance."

Introduction

Sailors understand both the importance and the difficulty in obtaining information on wind over oceans. The textbooks still describe global ocean wind distribution in sailor's terms: the calms of the Doldrums and Horse Latitudes, the steady Trade Winds, and the ferocity of the Roaring Forties. Just a few decades ago, almost all ocean wind measurements came from merchant ships. However, the quality and geographical distribution of these wind reports were uneven. Today, operational numerical weather prediction (NWP) also gives us wind information, but NWP depends on models, which are limited by our knowledge of the physical processes and the availability of data.

The ocean interacts with the atmosphere in nonlinear ways; processes at one scale affect processes at other scales. Adequate coverage can only be achieved from the vantage point of space. Space-based microwave sensors observe through clouds and measure ocean surface properties, backscatter, or emissivity, which are more directly related to stress than wind. The microwave scatterometer is the best-established instrument to measure surface stress magnitude and direction under clear and cloudy conditions, night and day, as described in the section "Scatterometry." Until the launch of the scatterometer, our knowledge of stress distribution was largely derived from winds. Wind and stress have been mixed up in the interpretation of these space-based measurements. The section "Wind and Stress Relation" helps us to understand their relation and makes better use of the scatterometer observations.

The primary functions of the radar altimeter, the synthetic aperture radar (SAR), and the microwave radiometer are not wind-stress measurements, but they give wind speed as a secondary product. Wind speed, even without direction, is important, and wind speed from these sensors can be applied with directional information derived from other means. The polarimetric radiometer was also found recently to be sensitive to wind direction. The techniques of these sensors are briefly summarized in the section "Other sensors."

Scientific significance

Ocean wind is strongly needed for marine weather forecast and to avoid shipping hazards. Space-based wind measurements have been assimilated into operational NWP and used routinely in national centers for marine warning and forecasting. Surface wind convergence brings moisture and latent heat that drives deep convection and fuels hurricanes. The significance of wind measurement is clearly felt, for example, when a hurricane suddenly intensifies and changes course or when the unexpected delay of monsoon brings drought. Detailed distribution of wind power is also needed for the optimal deployment of floating wind farms in open sea that are enabled by new technologies (Liu et al., 2008a).

Wind-induced stress drives ocean current (ageostrophic component) and generates wave. The two-dimensional stress field is needed to compute the divergence and curl (vorticity) that control the vertical mixing. The mixing brings short-term momentum and heat trapped in the surface mixed layer into the deep ocean, where they are stored over time. It also brings nutrients and carbon stored in the deep ocean to the surface, where there is sufficient light for photosynthesis. The horizontal currents, driven in part by stress, distribute the stored heat and carbon in the ocean. Stress affects the turbulent transfer of heat, moisture, and gases between the ocean and the atmosphere and is critical in understanding and predicting weather and climate changes.

Relations between wind and stress

Ocean surface stress (τ) is the turbulent transfer of momentum generated by atmospheric instability caused both by wind shear (difference between wind and current) and buoyancy (vertical density stratification resulting from temperature and humidity gradients). Direct τ measurement has only been done in a few field campaigns in the past. For all practical purposes, our knowledge of τ is derived from winds (U) at a reference height through a drag coefficient C_D, which is defined by

$$\tau = \rho C_D (U - U_S)^2 \tag{1a}$$

where U_s is the surface current and ρ is the air density.

In a similar fashion, the turbulent fluxes of heat (H) and moisture (E) have been related to the mean parameters – wind speed U, potential temperature T, specific humidity Q at 10 m, and sea surface temperature T_s, through

$$H = \rho C_P C_H (T - T_s)(U - U_S) \tag{2a}$$

$$E = \rho C_E (Q - Q_s)(U - U_S) \tag{3a}$$

where c_P is the isobaric specific heat. The mean parameters are the measurements generally available from routine ship reports. In the past, the transfer coefficients, C_H and C_E, were approximated with the same values as C_D.

The transfer coefficient has been derived largely in field campaigns. Figure 1, from Liu et al. (1979), illustrates the behavior of C_D at neutral stability. At low wind speed ($U < 3$ m/s), the flow is smooth; C_D increases with decreasing wind speed. And at moderate wind $3 < U < 25$ m/s, C_D is an increasing function of wind speed for a rough sea with open fetch. Stability and surface roughness are the main factors affecting the variability of the coefficients. Secondary factors, such as sea states and spray from breaking waves, whose data are not generally available are not included in these parameterization schemes and should be part of the errors (e.g., Bourassa et al., 1999).

Liu et al. (1979) first postulated that, in a rough sea, under a moderate range of winds, C_H and C_E do not increase with wind speed because of molecular constraint at the interface, while C_D may still increase because momentum is transported by form drag. Liu's hypothesis, as illustrated in Figure 1, was subsequently supported by measurements in field experiments (e.g., DeCosmo et al., 1996).

Emanuel (1995) argued, from theoretical and numerical model results, that the scenario of Liu et al. (1979) could not hold at the strong wind regime of a hurricane. To attain the wind strength of a hurricane, the energy dissipated by drag could not keep increasing while the energy fed by sensible and latent heat does not increase with wind speed. His argument puts limit on the increase of C_D as a function of wind speed. The postulation of the level-off of the increase of C_D with wind speed at hurricane scale winds was supported by the results of the laboratory studies of Donelan et al. (2004) and the aircraft experiments by Powell et al. (2003), as illustrated in Figure 2. The result of Large and Pond (1981), derived for the range of moderate wind speeds, is extrapolated to the range of strong wind speeds for comparison in the figure. The high wind behavior of C_D may post constrain in retrieving hurricane scale winds by the scatterometer.

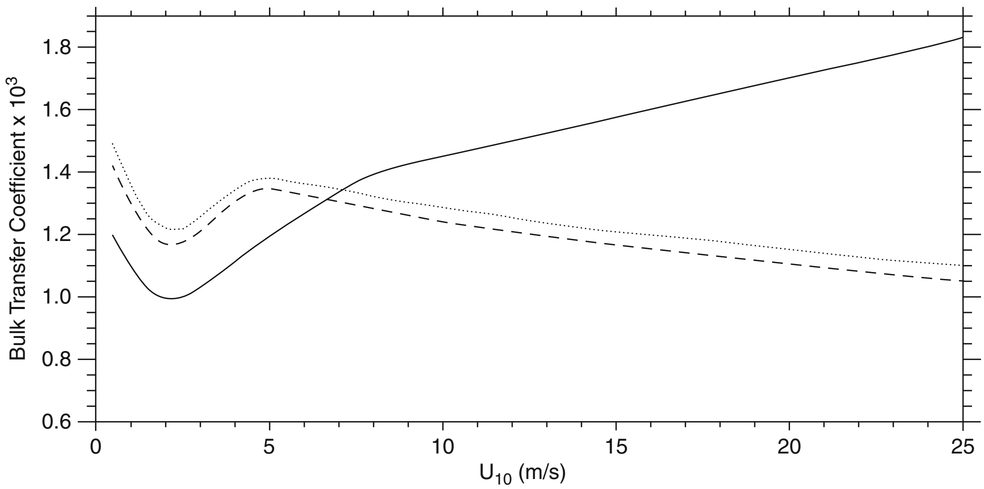

Sea Surface Wind/Stress Vector, Figure 1 Variation of the bulk transfer coefficients of momentum (drag coefficient), heat, and moisture with wind speed by Liu et al. (1979).

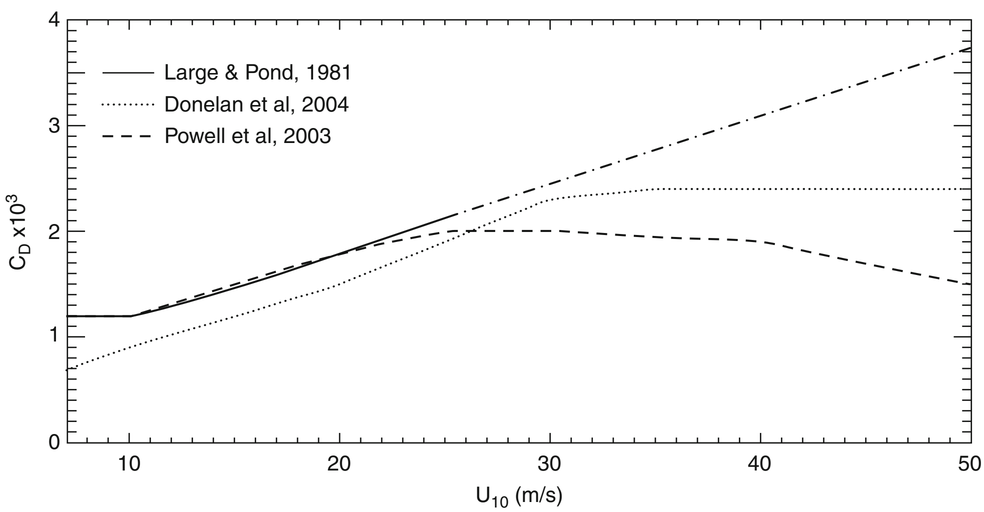

Sea Surface Wind/Stress Vector, Figure 2 Variation of the drag coefficients in strong winds.

Liu et al. (1979), for the first time, performed the bulk parameterization of the surface fluxes by solving the nondimensional flux-profile relations (also called similarity functions), thus including the effects of stability and surface molecular constraints. The functions are:

$$\frac{U - U_s}{U_*} = 2.5(\ln\frac{z}{z_0} - \psi_U) = \frac{1}{\sqrt{C_D}} \tag{1b}$$

$$\frac{T - T_s}{T_*} = 2.5(\ln\frac{z}{z_T} - \psi_T) = \frac{\sqrt{C_D}}{C_H} \tag{2b}$$

$$\frac{Q - Q_s}{Q_*} = 2.5(\ln\frac{z}{z_Q} - \psi_Q) = \frac{\sqrt{C_D}}{C_E} \tag{3b}$$

where $U_* = (\tau/\rho)^{1/2}$ is the frictional velocity; T_* and Q_* are nondimensional flux parameters defined as $T_* = H/(C_P U_*)$ and $Q_* = E/(U_*)$; z_0, z_T, and z_Q are the roughness lengths; and φ_U, φ_T, and φ_Q are functions of the stability parameter, which is the ratio of buoyancy to shear production of turbulence. When U_s and φ_U are zero, U becomes the equivalent neutral wind (U_N), which is uniquely related to U_* (or τ). U_N has been used as the geophysical product of the scatterometer.

Typical wind profiles at various stabilities are shown in Figure 3. The atmosphere is rarely exactly neutral. Even when there is no vertical temperature gradient, there is likely to be a humidity gradient. To compute U_N from conventional wind measurements of U (A on the blue

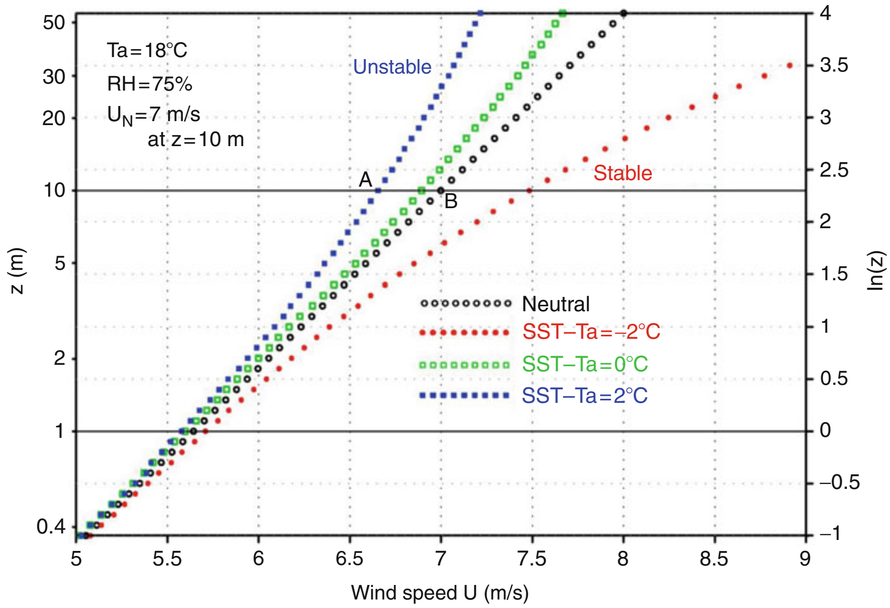

Sea Surface Wind/Stress Vector, Figure 3 Typical wind profiles at various stability conditions derived from the flux-profile relation by Liu et al. (1979). B is the equivalent neutral wind corresponding to the actual wind measurement at A.

curve in Figure 3), U_* and z_0 are computed as the slope and intercept at the surface of the curve. The neutral relation (straight line) defined by U_* and z_0 will give U_N (point B). This method has been used in algorithm development and calibration of all scatterometers launched by NASA. At a given level, U_N is larger than the actual wind (U) under unstable conditions but lower under stable condition. From Equation 1b, $U_N\text{-}U = 2.5U_*\psi_U$, assuming the dependence of z_0 on buoyance is much smaller than on wind shear. This difference is the inherent error of using scatterometer measurement as the actual wind. While the parameterization method by Liu et al. (1979) has been improved (e.g., Fairall et al., 1996), the formulation of ψ was largely based on experimental data taken on land, validated only with small amount of measurements over ocean, and may still have considerable uncertainties.

Scatterometry

During the Second World War, marine radar operators observed noises on their radar screens, which obscured small boats and low-flying aircraft. They termed this noise "sea clutter." This clutter was the backscatter of the radar pulses by the small waves on the ocean's surface. The radar operators at that time were quite annoyed by this noise, not knowing that a few decades later, scientists would make important use of it.

Scatterometers send microwave pulses to the Earth's surface and measure the power backscattered from the surface roughness. The roughness may describe the characteristics of polar ice or vegetation over land. Over the ocean, which covers over three quarters of the Earth's surface, the surface roughness is largely due to the small centimeter wavelength waves on the surface. These surface waves are believed to be in equilibrium with the local stress. The backscatter depends not only on the magnitude of the stress but also the stress direction relative to the direction of the radar beam (azimuth angle). The capability of measuring both stress magnitude and direction is the major, important characteristic of the scatterometer. Liu and Large (1981) were first to relate scatterometer and direct stress measurements.

There are far fewer stress than wind measurements for validation and calibration, and the equivalent neutral wind (U_N) is used as the geophysical product of the scatterometer (Liu and Tang, 1996). By definition, U_N is uniquely related to τ, while the relation between τ and U depends on atmospheric stability, as discussed in the previous section. U_N is similar to U_* and can be viewed as stress in wind units.

At incident angles greater than 20°, the radar return is governed by Bragg scattering, and the backscatter increases with U_N. The backscatter is governed by the inphase reflections from surface waves. The geophysical model function (GMF), from which U_N is retrieved from the observed backscatter, in form of the normalized radar cross section (σ_o), is largely based on empirical fits of data. The symmetry of backscatter with respect to wind direction requires observations at multiple azimuth angles to resolve the directional ambiguity. Because of the uncertainties in the wind retrieval algorithm and noise in the backscatter measurements, the problem with directional ambiguity was not entirely eliminated even with three

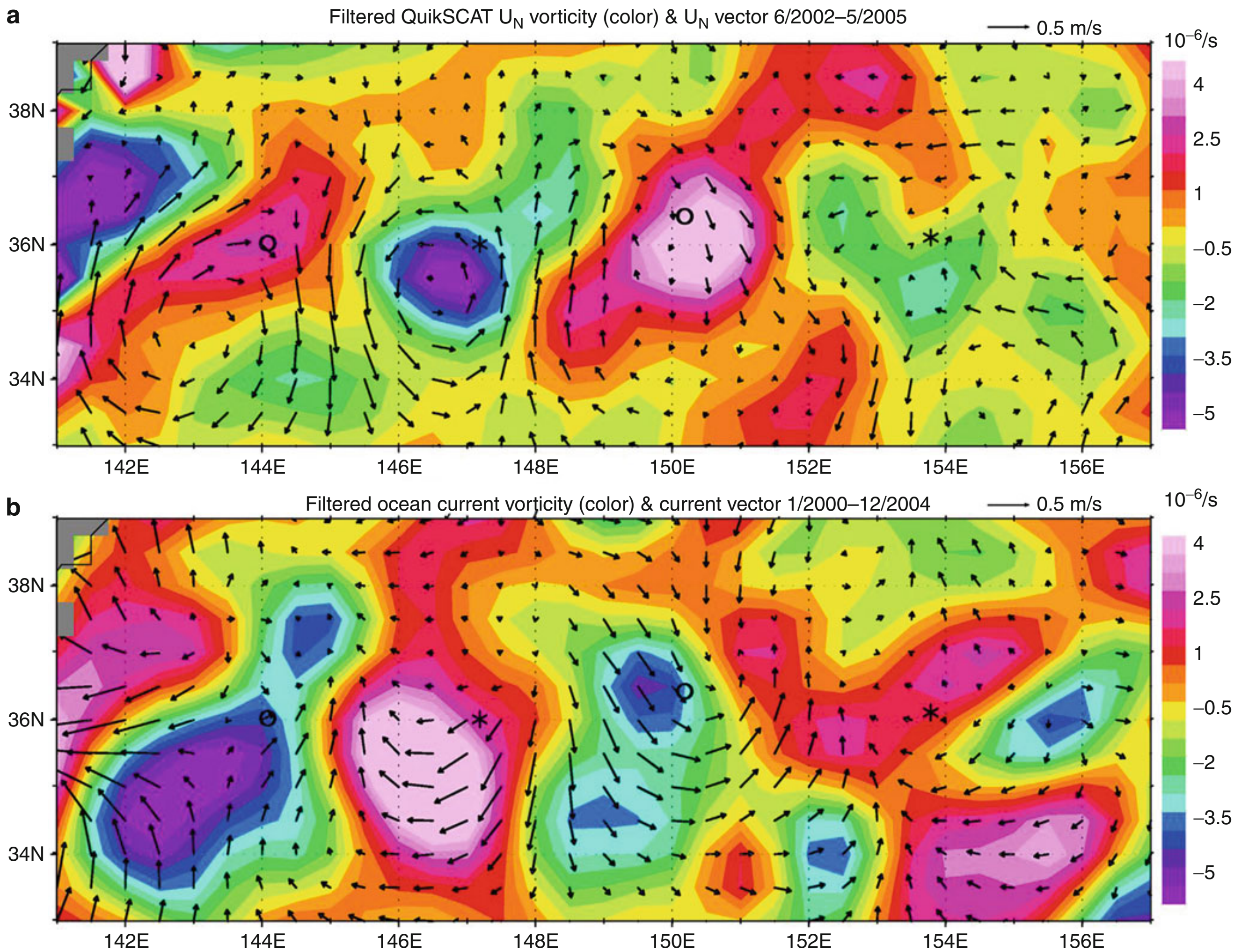

Sea Surface Wind/Stress Vector, Figure 4 (**a**) Filtered vector (*black arrows*) superimposed on vorticity (color, 10^{-6} s^{-1}) of U_N observed by QuikSCAT. (**b**) Filtered vector (*black arrows*) superimposed on vorticity of the surface current measured by Lagrangian drifters.

azimuthal looks in the scatterometers launched after Seasat. A median filter iteration technique has been commonly used to remove the directional ambiguity.

Although scatterometers are known to measure surface stress, they have been used and promoted as wind measuring instruments and U_N has been used as the actual wind, particularly in operational weather applications. This is justified on the assumption that, over the large expanse of ocean, ocean current is weak compared with wind and the atmosphere is under near neutral conditions. Over the Agulhas Extension and the Kuroshio Extension current with sharp horizontal current shear and temperature gradients, however, Liu et al. (2007) and Liu and Xie (2008) show that stress could be very different from winds. Over the current meanders, one would expect that the wind will be dragged in the direction of the current. Figure 4 clearly shows that where the vorticity of U_N measured by QuikSCAT is positive, the vorticity of the surface current measured by the drifters is negative and vice versa, indicating almost opposite rotations. This is a clear indication that the scatterometer measurement has the characteristic of turbulent stress generated by shear rather than wind. The directional difference between scatterometer measurement and current exists because the scatterometer measures stress, which is the vector difference between wind and current (Park et al., 2006).

The ubiquitous spatial coherence between sea surface temperature (T_s) and U_N measured by the scatterometer found under a variety of atmospheric conditions is also the characteristics of turbulent stress generated by buoyancy. In the unstable region, atmospheric buoyancy generates turbulent momentum transport and increases the stress magnitude. Figure 5a shows the coherence over the Kuroshio Extension. Figure 5b shows similar

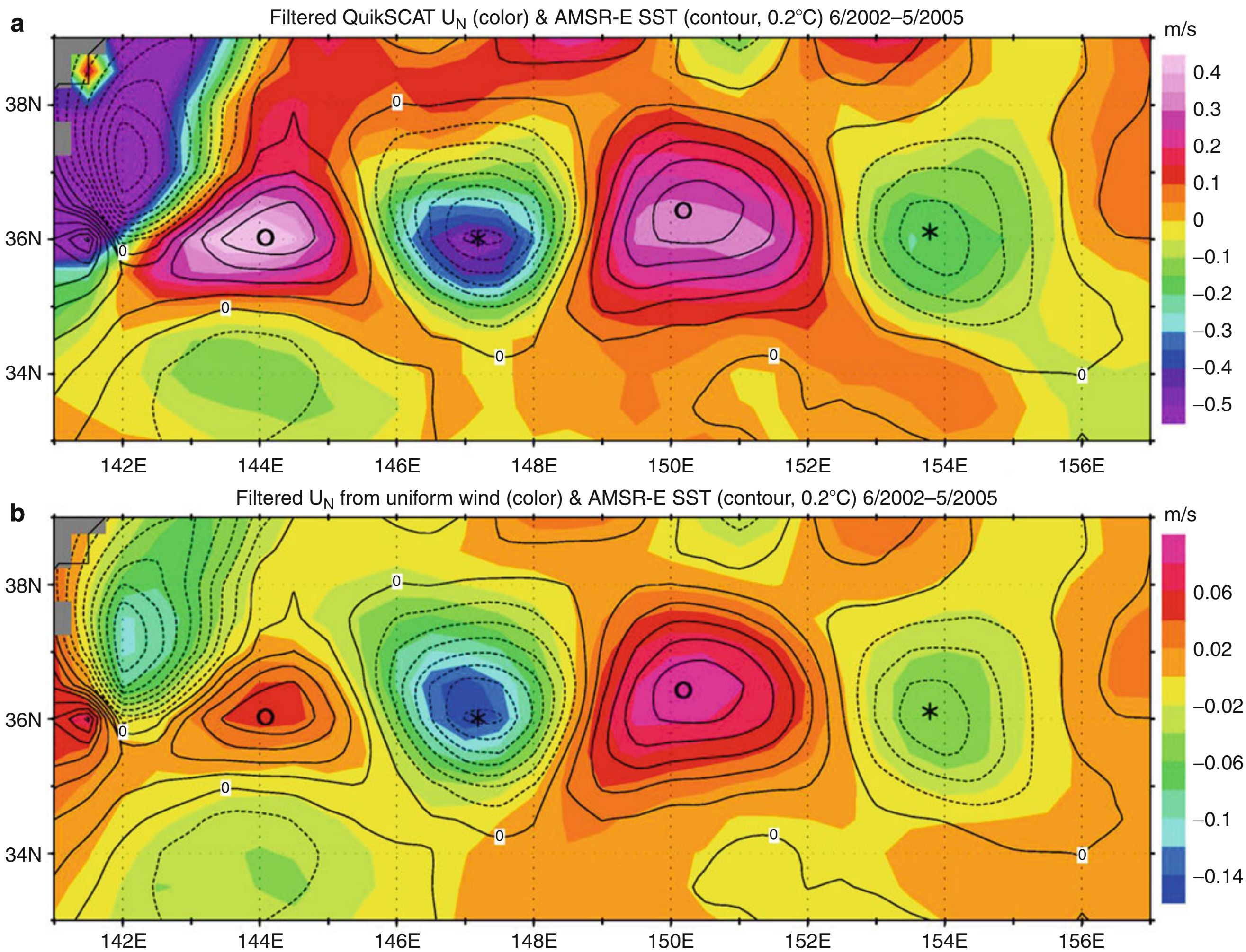

Sea Surface Wind/Stress Vector, Figure 5 Isotherms of filtered Ts measured by AMSR-E (0.2 °C interval) superimposed on (**a**) filtered magnitude of QuikSCAT U_N (color, m/s), and (**b**) filtered U_N computed from a uniform wind field of u = 7.5 m/s. Solid and broken lines represent positive and negative values, respectively.

coherence between T_s and U_N computed from a uniform wind field under similar stability condition, demonstrating that the coherence is the characteristic of stress and not wind. Factors affecting larger-scale wind, such as pressure gradient force, Coriolis force, and baroclinicity, are not important at the small scales of turbulence, and that is the reason of ubiquitous coherence under various atmospheric conditions. The higher stress over warmer water affects atmospheric wind aloft, but the influence will be subjected to these large-scale factors. Ocean parameters, such as surface current and temperature, are needed to derive wind from stress in these frontal regions.

Retrieving strong winds from the scatterometer measurements is also difficult. The problem is obvious in Figure 6, derived from NASA's scatterometer on QuikSCAT measuring at Ku-band. Data for the 12 hurricanes in the North Atlantic in the 2005 seasons, excluding those with over 10 % chances of rain, were examined. Figure 6 shows that, in moderate winds ($U < 35$ m/s), the logarithm of σ_o (in db) increases linearly with the logarithm of wind speed, at both polarizations. At strong winds ($U > 35$ m/s), however, σ_o increases at a much slower rate with increasing wind speed. Similar saturation is found in the European Advanced Scatterometer (ASCAT), measuring at C-band. Such high wind saturation has also been observed from aircraft flying over hurricanes.

When the model function developed over the moderate wind range is applied to the strong winds, an underestimation of wind speed results. Strong efforts have been made to adjust the model function (slope in Figure 3) in strong winds and to find the right channel (combination of polarization, frequency, incident angle) that would be sensitive to the increase of strong winds (e.g., Fernandez et al., 2006). The success would be difficult if flow separation occurs at high winds and the surface roughness and stress

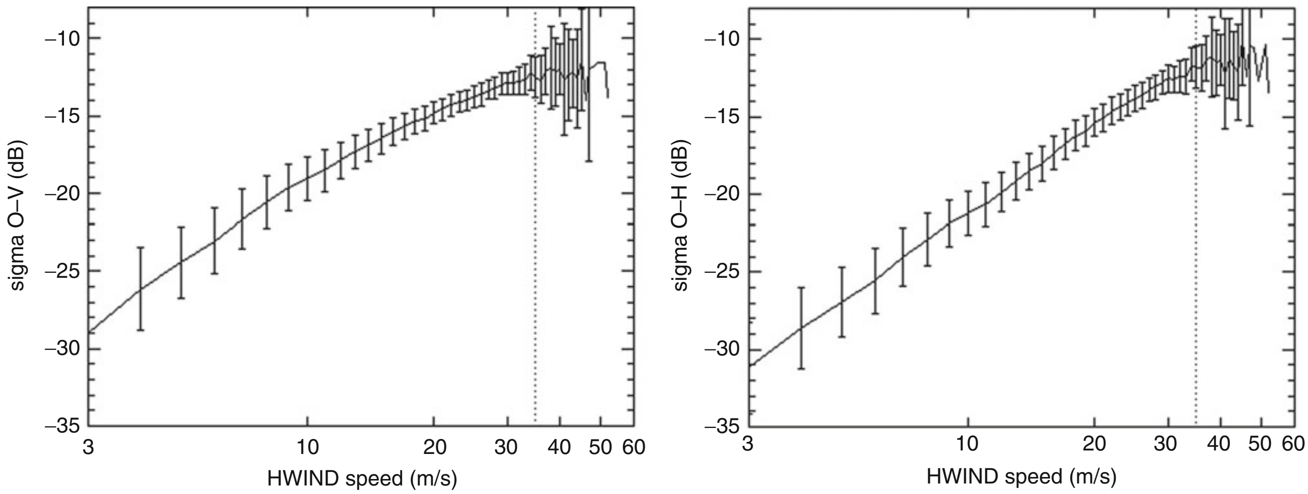

Sea Surface Wind/Stress Vector, Figure 6 Normalized radar cross section at two polarizations measured by QuikSCAT for 12 hurricanes as a function of colocated surface wind provided by the National Hurricane Center.

do not increase with winds as discussed in section "Relations between wind and stress."

Direct stress retrieval

Weissman and Graber (1999) made an early attempt to build a GMF to retrieve stress instead of wind. There are many reasons for a GMF-S (stress) to retrieve stress (or U_*) directly rather than the present GMF-W to retrieve U_N. The first reason is the deficiency of the present GMF-W, which should be developed and calibrated with U_N computed from research quality in situ wind measurements, as described in the section "Relations between wind and stress." Such computation of U_N from in situ measurements was performed before credible ocean surface wind products became available from operational NWP centers. Most of the tuning of the revised GMF after Seasat was based on NWP products that are not U_N (not corrected for stability dependence). The resultant errors are not reversible and difficult to gauge.

The second reason is the uncertainty of the drag coefficient. Ideally, stress could be derived from U_N retrieved from the scatterometer, using a neutral drag coefficient. However, if the drag coefficient is not the same as that was used to derive U_N for development of the GMF, error will be introduced through the uncertainty of drag coefficient.

The other two reasons are related to the directional difference between wind and stress. The procedure to "select" the stress direction should be different from wind direction in two ways. In the first way, we should initialize the ambiguity removal process with "nudging" fields that are more relevant to stress than wind. Where a strong ocean current exists, the stress should point to the direction of the vector difference between wind and current. The second way is to develop a flexible median filter to accommodate the small spatial scale of stress as compared with winds. One of the problems of the selection is the lack of sufficient current information.

One of the reasons usually given for promoting scatterometer as a wind sensor instead of a stress sensor is that there is more wind than stress measurements to develop and calibrate the GMF. Such an explanation is not valid because U_N, by definition, has an unambiguous relation with stress and needs stress for computation. To provide each U_N for development or calibration of the GMF from measured wind U, stress or U_* has to be computed first as discussed in the section "Relations between wind and stress."

The stress derived from wind in such a way is not ideal because it addresses only the stability problem but does not include current information. Such deficiency may be somewhat alleviated through the ambiguity removal process by using more appropriate filter size and nudging with the vector difference between wind and optimal surface current information that is available. The direct retrieval of stress depends not only on the fast and large-scale atmospheric circulation but also on the small-scale and slow ocean processes, as reflected in surface current and temperature.

Other sensors

Both the microwave altimeter and SAR are similar to the scatterometer in the sense that they are active sensors that send microwave pulses to the Earth's surface and measure the backscattered power. The microwave radiometer is a passive sensor, observing the radiance emitted by the Earth and its atmosphere.

While the scatterometer views at oblique angles, the altimeter views at nadir (very small incident angles). At nadir, the backscattered energy is a result of specular reflection (the wavelets serve as small mirrors), and the backscatter is not sensitive to U_N direction. Because the instrument is not scanning, data are only available at very narrow (2 km) repeated ground tracks. The coverage of all the past altimeters is poor compared with the scatterometer and the microwave radiometers.

A SAR looks perpendicular to aircraft path only at one azimuth angle and cannot resolve the U_N direction like the scatterometer. SAR has spatial resolutions that are much better than scatterometers, but the high resolution also introduces higher uncertainties in accuracy caused by secondary effects that affect surface roughness. The instrument and the data processing procedure are much more complicated than the scatterometer. The scatterometer GMF can be used to relate the σ_o measured by SAR to U_N. However, a particular value of σ_o may correspond to a range of U_N, depending on the azimuth angle. Hence, in order to retrieve U_N with the GMF, the U_N direction must first be specified. Whether the a priori direction information is derived from the orientation of km-scale structure in the SAR image or from operational NWP models, the spatial scales are much coarser than those of σ_o.

Ocean surface wind speed has also been derived from the radiance measured by a microwave radiometer. It is generally believed that wind speed affects the surface emissivity indirectly through the generation of ocean waves and foam. Radiometers designed to observe the ocean surface operate primarily at window frequencies, where atmospheric absorption is low. Radiances at frequencies sensitive to sea surface temperature, atmospheric water vapor, and liquid water are also measured; they are used to correct for the slight interference by the atmosphere. It was demonstrated in several airborne experiments (e.g., Yueh et al., 1997) that the polarization properties of the sea surface emission vary not only as a function of the wind speed but also as a function of wind direction. The wind direction measuring capability is being tested by a polarimetric radiometer, WindSat on the Coriolis satellite, developed by the US Navy.

Potential improvements

Historically, the European Space Agency used the C-band (5 GHz), but NASA prefers the Ku-band (14 GHz) for their scatterometers. The backscatter at higher frequencies is more sensitive to shorter ocean waves. The Ku-band is more sensitive to weak wind-stress variations but is more subject to atmospheric effects and rain contamination. Attempts have been made to retrieve winds from L-band (1.4 GHz) scatterometer on Aquarius (Yueh et al., 2013). There have been calls for a multifrequency scatterometer that is sensitive to various parts of ocean surface wave spectrum and may reduce atmospheric and rain effects.

Present scatterometers are real-aperture systems and the spatial resolution is limited by the antenna size. A larger antenna will, of course, enhance the spatial resolution. Another way to achieve higher resolution is to add a synthetic aperture capability. One of the drawbacks of present scatterometers is the ambiguity in retrieving wind-stress direction. The backscatter is a cosine function of the azimuth angle. The correlation between co-polarized and cross-polarized backscatter is a sine function of azimuth angle. By adding polarized measurement capability to the scatterometer, the directional ambiguity problem could be mitigated.

One polar-orbiting scatterometer at a low-altitude (e.g., 800 km) orbit can sample at a location on Earth not more than two times a day. Additional instrument flying in tandem will allow the description of higher temporal variability and the reduction of the aliasing (bias introduced by subsampling) of the mean wind stress. As demonstrated by Liu et al. (2008b), adding ASCAT to QuikSCAT decreases the time required to cover 90 % of the Earth from 24 to 19 h. Adding Oceansat-2 of India resolves the inertial frequency desired by oceanographers and provides 6 hourly repeated coverage required by operational weather forecasters. The adverse effect due to the demise of QuikSCAT should be mitigated by data from WindSat or the scatterometer on Haiyang-2 of China. The scatterometer on Space Station will provide new sampling opportunity.

Not all space-based ocean surface wind and stress measurements are comparable in quality. Standardizing the technology requirements for observation accuracies of different research and operational applications and international cooperation are very desirable. Many scientific reports have affirmed the need for high-quality, continuous, and consistent long time series of ocean surface vector winds and stress.

Conclusion

The basics of scatterometry and air-sea turbulence transfer are reviewed to bring out the uniqueness of the scatterometer in measuring ocean surface stress in addition to wind. The ubiquitous spatial coherence of scatterometer measurements with ocean surface temperature and current is attributed to the two ocean factors that drive the buoyancy and wind-shear production of turbulence transfer (stress); the factors are less directly influential on wind. The reduced sensitivity of the scatterometer to the increase of wind speed at hurricane scale winds is related to the failure of conventional drag coefficient caused by flow separation. A scatterometer that measures stress better than wind is still important to the estimation of the dynamic forcing and the oceanic feedback that affects the maintenance and intensification of the storm. The feasibility, advantage, and need for a geophysical model function to retrieve stress directly rather than the equivalent neutral wind (the present geophysical product of the scatterometer) are explained. The direct retrieval of stress from scatterometer measurements will enable new science applications with a new perspective, as expounded by Liu et al. (2010).

Acknowledgments

This study was performed at the Jet Propulsion Laboratory, California Institute of Technology, under contract with the National Aeronautics and Space Administration (NASA). It was jointly supported by the Ocean Vector Winds, Ocean Surface Salinity, and Precipitation Measuring Mission Programs of NASA. Wenqing Tang provided valuable assistance.

Bibliography

Bourassa, M. A., Vincent, D. G., and Wood, W. L., 1999. A flux parameterization including the effects of capillary waves and sea state. *Journal of the Atmospheric Sciences*, **56**, 1123–1139.

DeCosmo, J., Katsaors, K. B., Smith, S. D., Anderson, R. J., Oost, W. A., Bumke, K., and Chadwick, H., 1996. Air-sea exchange of water vapor and sensible heat: the humidity exchange over the sea (HEXOS) results. *Journal of Geophysical Research*, **101**, 12001–12016.

Donelan, M. A., Haus, B. K., Reul, N., Plant, W. J., Stiassnie, M., Graber, H. C., Brown, O. B., and Saltzman, E. S., 2004. On the limiting aerodynamic roughness of the ocean in very strong winds. *Geophysical Research Letters*, **31**, L18306, doi:10.1029/2004GL019460.

Emanuel, K., 1995. Sensitivity of tropical cyclones to surface exchange coefficients and a revised steady state model incorporating eye dynamics. *Journal of the Atmospheric Sciences*, **52**, 3969–3976.

Fairall, C. W., Bradley, E. F., Rogers, D. P., Edson, J. B., and Young, G. S., 1996. Bulk parameterization of air-sea fluxes in TOGA COARE. *Journal of Geophysical Research*, **101**, 3747–3767.

Fernandez, D. E., Carswell, J. R., Frasier, S., Chang, P. S., Black, P. G., and Marks, F. D., 2006. Dual-polarized C- and Ku-band ocean backscatter response to hurricane-force winds. *Journal of Geophysical Research*, **111**, C08013, doi:10.1029/2005JC003048.

Large, W. G., and Pond, S., 1981. Open ocean momentum flux measurements in moderate to strong winds. *Journal of Physical Oceanography*, **11**, 324–336.

Liu, W. T., and Large, W. G., 1981. Determination of surface stress by Seasat-SASS: a case study with JASIN data. *Journal of Physical Oceanography*, **11**, 1603–1611.

Liu, W. T., and Tang, W., 1996. *Equivalent Neutral Wind*. Pasadena: JPL Publication 96–17, Jet Propulsion Laboratory. 16 pp.

Liu, W. T., and Xie, X., 2006. Measuring ocean surface wind from space. In Gower, J. (ed.), *Remote Sensing of the Marine Environment*, 3rd edn. Bethesda: American Society for Photogrammetry and Remote Sensing. Manual of Remote Sensing, Vol. 6, pp. 149–178. Chapter 5.

Liu, W. T., and Xie, X., 2008. Ocean–atmosphere momentum coupling in the Kuroshio extension observed from space. *Journal of Oceanography*, **64**, 631–637.

Liu, W. T., Katsaros, K. B., and Businger, J. A., 1979. Bulk parameterization of air-sea exchanges in heat and water vapor including the molecular constraints at the interface. *Journal of the Atmospheric Sciences*, **36**, 1722–1735.

Liu, W. T., Xie, X., and Niiler, P. P., 2007. Ocean–atmosphere interaction over Agulhas extension meanders. *Journal of Climate*, **20**, 5784–5797.

Liu, W. T., Tang, W., and Xie, X., 2008a. Wind power distribution over the ocean. *Geophysical Research Letters*, **35**, L13808, doi:10.1029/2008GL034172.

Liu, W. T., Tang, W., Xie, X., Navalgund, R., and Xu, K., 2008b. Power density of ocean surface wind-stress from international scatterometer tandem missions. *International Journal of Remote Sensing*, **29**, 6085–6090.

Liu, W. T., Xie, X., and Tang, W., 2010. Scatterometer's unique capability in measuring ocean surface stress. In Barale, V., Gower, J. F. A., and Alberotanza, L. (eds.), *Oceanography from Space*. New York: Springer, pp. 93–111. Chapter 6.

Park, K.-A., Cornillon, P., and Codiga, D. L., 2006. Modification of surface winds near ocean fronts: effects of the Gulf Stream rings on scatterometer (QuikSCAT, NSCAT) wind observations. *Journal of Geophysical Research*, **111**, C03021, doi:10.1029/2005JC003016.

Powell, M. D., Vickery, P. J., and Reinhold, T., 2003. Reduced drag coefficient for high wind speeds in tropical cyclones. *Nature*, **422**, 279–283.

Weissman, D. E., and Graber, H. C., 1999. Satellite scatterometer studies of ocean surface stress and drag coefficients using a direct model. *Journal of Geophysical Research*, **104**(C5), 11329–11335.

Yueh, S. H., Wilson, W. J., Li, F. K., Nghiem, S. V., and Ricketts, W. B., 1997. Polarimetric brightness temperatures of sea surfaces measured with aircraft K- and Ka-band radiometers. *IEEE Transactions on Geoscience and Remote Sensing*, **35**, 1177–1185.

Yueh, S. H., Tang, W., Fore, A. G., Neumann, G., Hayashi, A., Freedman, A., Chaubell, J., & Lagerloef, G. S. E., 2013. L-band passive and active microwave geophysical model functions of ocean surface winds and applications to Aquarius retrieval. *IEEE Transactions on Geoscience and Remote Sensing*, **51**, 4619–4632. See http://ieeexplore.ieee.org/xpl/articleDetails.jsp?tp=&arnumber=6553597&url=http%3A%2F%2Fieeexplore.ieee.org%2Fxpls%2Fabs_all.jsp%3Farnumber%3D6553597.

Cross-references

Climate Data Records
Microwave Surface Scattering and Emission
Radar, Scatterometers
Radiation, Polarization, and Coherence
Severe Storms
Tropospheric Winds
Water and Energy Cycles

SEVERE STORMS

Charles A. III Doswell
Doswell Scientific Consulting, Norman, OK, USA

Synonyms

Severe convection; Severe local storms; Severe weather

Definition

Severe storms. Any deep convective storm, usually associated with lightning and thunder, that produces one or more of the following: large hailstones, strong winds, and/or tornadoes. For the United States, the threshold diameter for severe hail is 2.54 cm (1 in.) and the threshold speed for severe winds is 25 m s^{-1} (50 knots), but *any* tornado is considered severe (tornadoes are ranked in six categories according to the *Enhanced Fujita scale* (Fujita, 1971), ranging from EF0 to EF5). In many countries,